

A MODEL OF LOCAL DISTRIBUTION OF SATURATION IN A FRACTURED LAYER, AND ITS APPLICATION

Yuichi NIIBORI and Tadashi CHIDA

Department of Resource Engineering,
 Faculty of Engineering, Tohoku University
 Sendai 980, Japan

ABSTRACT

This paper describes a model of local distribution of liquid water (or steam) saturation in a fractured layer. The model, based on the Bernoulli trials as a probability density function of saturation, gives the following relation between the average value of the relative permeability for the water phase, k_{rwa} , and the arithmetical mean of saturation, S_{wa} :

$$k_{rwa} = S_{wa}^m,$$

where m is an index representing the non-uniformity of saturation ($1 < m < 4$). When $m=4$, the saturation is distributed uniformly. The proposed model also gives the average value for the relative permeability of the steam phase, k_{rga} , as follows:

$$k_{rga} = 1 - S_{wa}^m - 2S_{wa} + 2S_{wa}^{(2m+1)/3}.$$

These relations are applied to analysis of some experimental data already reported by the authors. Also, this presentation shows the validity of the Bernoulli trials as a density probability function of saturation in comparison with other kinds of such functions: the normal distribution, the triangle distribution and the beta distribution.

INTRODUCTION

The relative permeability, k_r , plays an important role in analyzing two-phase flow through a porous medium, because k_r determines the velocity of each phase, v_i , according to $v_i = -k_r k \nabla p / \mu_i$, where k is the absolute permeability (constant in time), μ is viscosity, ∇p is gradient of pressure and the subscript i refers to phase of water (w) or steam (g). In general, k_r is expressed by a function of water saturation, S_w (Grant et al., 1982, p289). However, S_w is not always distributed uniformly, even if the space considered in evaluating the value of S_w is a unit of discrete region in the numerical analysis. Because a geothermal reservoir is composed of innumerable cracks. The authors have investigated about relative permeabilities (Niibori & Chida, 1989, 1992, 1994), for such flow system.

This presentation indicates a model of local distribution of S_w , using the Bernoulli trials as a probability

density function of S_w . The model gives correlation equations between the relative permeabilities and the arithmetical mean of S_w in the local distribution. Validity of the model is investigated through experimental data.

MODELING SATURATION DISTRIBUTION

In the first place, let us consider a simple problem on local distribution of the saturation. Now assume that the two values of water saturation, $S_{w1}=0$ and $S_{w2}=1$ in the flow path 1 and 2, respectively, in a spatial region. Then, the average relative permeability, k_{rwa} , of liquid water phase (here in after, referred as water phase) in the region is calculated as follows:

$$k_{rwa} = (k_{rw1} + k_{rw2})/2 = 0.5, \quad (1)$$

where k_{rw1} and k_{rw2} are the relative permeabilities of the path 1 and 2, respectively. On the other hand, we have the following Corey's equation:

$$k_{rw} = S_w^4. \quad (2)$$

As the arithmetical mean of the path 1 and 2 is

$$S_{wa} = (S_{w1} + S_{w2})/2 = 0.5, \quad (3)$$

it is also possible to calculate the relative permeability, k_{rwa} , by substituting S_{wa} to Equation (2):

$$k_{rwa} = 0.5^4 = 0.0625. \quad (4)$$

Consequently, we have the two kinds of relative permeabilities, k_{rwa} and k_{rw} , which are different from each other. This discrepancy suggests that the relation between relative permeabilities and saturation depends not only on the average of saturation but also its distribution, apparently.

To estimate the relative permeabilities considered local distribution of saturation, the saturation is assumed to be described by a suitable probability density function, $F(S_w)$, as shown in Figure 1. In general, we can assume that in a spatial region of several cm, as shown in Fig.1 (1), (2) and (3), Darcy's law and the concept of relative permeability (also, saturation) are established. On the contrary, in

a unit (e.g., Δx) of discrete region, whose size is about 10m through 1km in the numerical analysis, S_w is not always distributed uniformly.

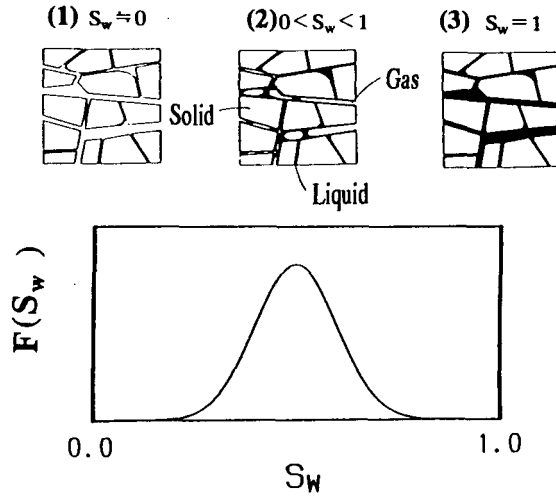


Figure 1 Illustration of Local Distribution of saturation.

Using such a probability density function, $F(S_w)$, Niibori & Chida (1989) defined the average, relative permeabilities, k_{rwa} and k_{rga} , respectively, as follows:

$$k_{rwa} = \frac{\int_0^1 F(S_w) k_{rw} dS_w}{\int_0^1 F(S_w) dS_w}, \quad (5)$$

$$k_{rga} = \frac{\int_0^1 F(S_w) k_{rg} dS_w}{\int_0^1 F(S_w) dS_w}. \quad (6)$$

(here in after, k_{rwa} and k_{rga} are referred as the apparent relative permeability). Then the arithmetical mean of saturation is

$$S_{wa} = \frac{\int_0^1 F(S_w) S_w dS_w}{\int_0^1 F(S_w) dS_w}. \quad (7)$$

As for k_{rw} and k_{rg} (not k_{rwa} and k_{rga}), we use the empirical equations, Eq.(2) and the following equation, which have been widely used in geothermal reservoir analyses by; for example, Faust & Mercer (1979), Zvoloski et al. (1980), Sorey et al. (1980), Pruess et al. (1983), O'Sullivan et al. (1985), Gudmundsson et al. (1986) and Niibori et al. (1987):

$$k_{rg} = (1 - S_w)^2 (1 - S_w^2), \quad (8)$$

where S_w is the normalized saturation (Aziz & Settari, 1979, p.33) considering the residual saturations of water and gas phases in the strict sense.

Niibori & Chida (1992) investigated relationships between k_{rw} and S_{wa} , assuming some kinds of probability density function of saturation, the Beta distribution, the triangle distribution, the normal distribution and the Bernoulli trials, because it is impossible to determine the probability density function a prior. The results suggest that the average relative permeabilities depend not on kind of such function, but on the arithmetical mean, the standard deviation, σ , and the skewness μ_3/σ^3 of saturation as follows:

$$\sigma^2 = \frac{\int_0^1 F(S_w) (S_w - S_{wa})^2 dS_w}{\int_0^1 F(S_w) dS_w}, \quad (9)$$

$$\mu_3 = \frac{\int_0^1 F(S_w) (S_w - S_{wa})^3 dS_w}{\int_0^1 F(S_w) dS_w}. \quad (10)$$

For example, the apparent relative permeabilities based on the Beta distribution agree quit well with those on the Bernoulli trials, when the values of S_{wa} , σ and μ_3/σ^3 each coincide with those of the Beta distribution. Such tendency is appeared, even if the probability function is described by any type function (the Beta distribution, the Normal distribution, the triangle distribution, and the Bernoulli trials).

Figure 2(a) displays the regions of k_{rwa} and k_{rga} , given by the Beta distribution (with one peak), also comparing the experimental data already reported by Wyckoff & Botset (1936). In the same way, Figure 2(b) shows the regions given by the Bernoulli trials (representing a probability density function with two peaks). These figures suggest that some experimental data are accompanied with the saturation distribution with relatively small value of the standard deviation, because its maximum value for the Beta distribution is smaller than that for the Bernoulli trials under the condition of $0 \leq S_w \leq 1$.

The Bernoulli trials are composed of S_{w1} , S_{w2} ($0 \leq S_{w1} \leq S_{w2} \leq 1$) and f (which is ratio of S_{w2} , thus the ratio of S_{w1} is $1-f$), as shown in Figure 3. To derive correlation equations between k_{rg} and S_{wa} for the water- and the gas-phase, respectively, we assume such a distribution as Figure 4. This figure shows an illustration of the saturation distribution on the radial direction, considering the heat exchange surface locally in a fractured layer. In such a case, we assume the smaller saturation S_{w1} to be zero, that is:

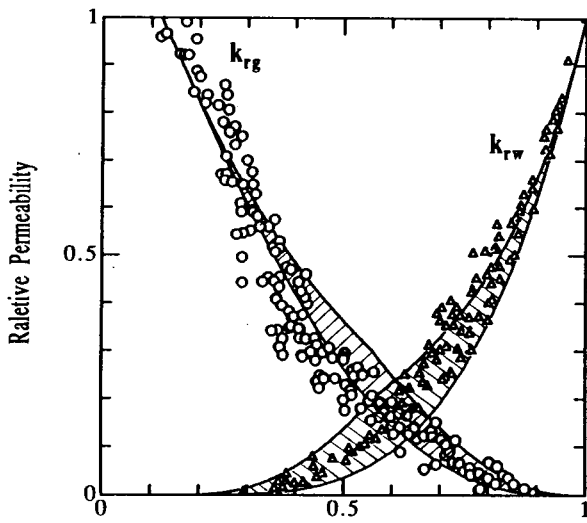
$$S_{w1} = 0, \quad (11)$$

because the region, close to the heat exchange surface, is occupied with the steam-phase. On the other hand, when S_{w2} is described as follows:

$$S_{w2} = S_{wa}^{(m-1)/3}, \quad (12)$$

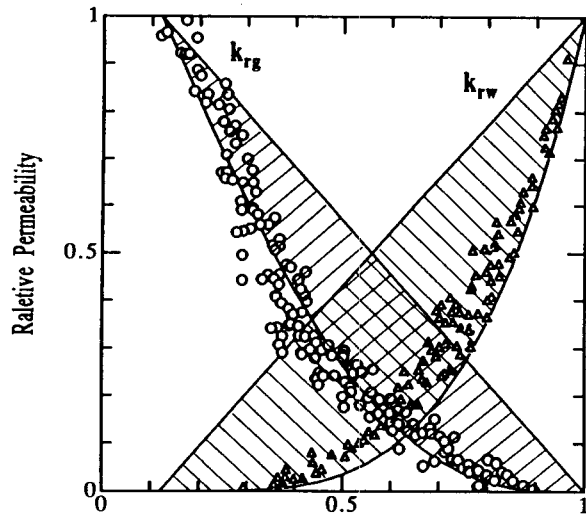
the model of local distribution of saturation gives

$$k_{rwa} = S_{wa}^m, \quad (13)$$



Water Saturation

(a)



Water Saturation

(b)

Figure 2 Application of the apparent relative permeability, based on (a) the Beta distribution and on (b) the Bernoulli trials, to the experimental data.

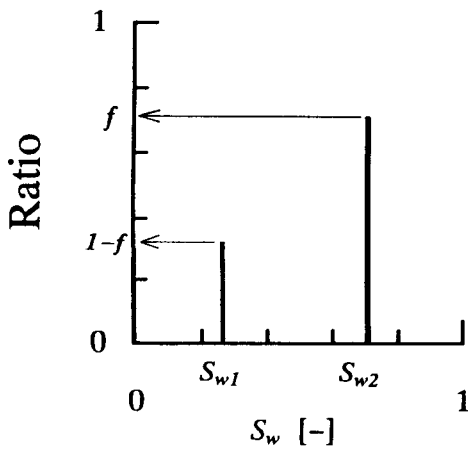


Figure 3 Illustration of the Bernoulli trials.

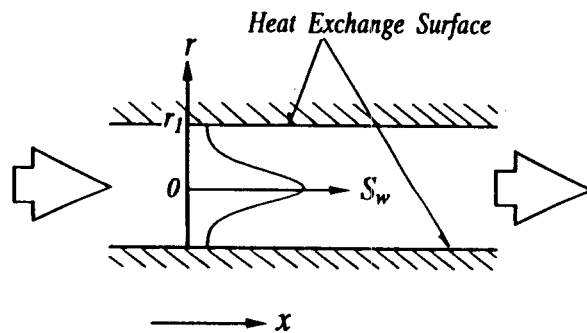


Figure 4 Modeling saturation distribution.

where S_{wa} is the arithmetical mean of the water saturation. Then, the value of f is described by

$$f = S_{wa}^{(4-m)/3} \quad (14)$$

m is an index representing the non-uniformity of saturation ($1 < m < 4$). When $m=4$, the saturation is distributed uniformly. The proposed model also gives the average value for the relative permeability of the steam phase, k_{rga} , as follows:

$$k_{rga} = 1 - S_{wa}^m - 2S_{wa} + 2S_{wa}^{(2m+1)/3} \quad (15)$$

Figure 5 shows the relation between S_{wa} and k_{ra} for each m (Fig.5(a) is for the water-phase, and Fig.5(b) is for the steam-phase.) From Figs.5(a) and (b), we can recognize that Eqs.(13) and (15), respectively, describe conveniently the regions of k_{ra} indicated by Fig.2(b) for water- and steam-phase.

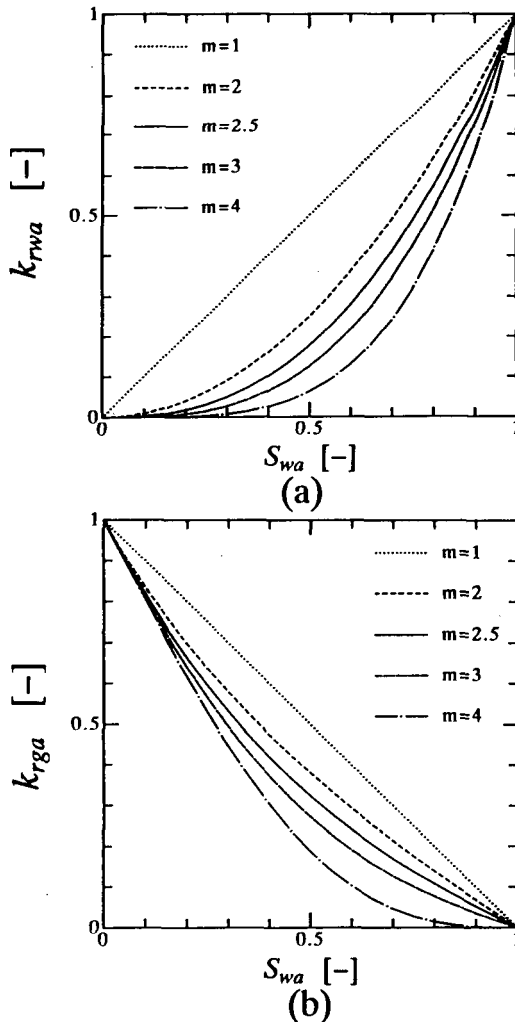


Figure 5 Correlation curves of apparent permeabilities to the arithmetical mean of saturation for (a) water-phase and (b) steam-phase.

APPLICATION

Experiments

The experiments are carried out by using a packed glass beads bed submerged horizontally in a thermostat at a temperature of more than 373K (Niibori et al., 1992). Figure 6 shows a schematic diagram of an experimental apparatus. Hydrostatic heads at the inlet and the outlet are fixed by overflows, respectively. Water is injected continuously into the bed under a constant pressure gradient and is heated from the surrounding, and part of the water vaporizes in the bed. When the temperature and the flow rates of steam and hot water attain to the steady state, 0.5cm^3 of ammonia water solution (about five volume percent of NH_3) is injected into the bed as a tracer. The tracer vaporizes in the bed, and ammonia gas flows out of the bed with steam. Then, the NH_3 content in the exit gas is measured by a gas chromatography every few minutes to evaluate the tracer response. Temperature in the bed is measured by thermocouples and an AD converter. Flow rates of water and steam at the outlet are also measured by a separator, a cooler and two electric balances. These data are stored to a magnetic disc through a personal computer every 15 seconds. Table 1 summarizes the experimental conditions.

Table 1 Experimental conditions

length of the packed bed	145mm, 290mm
Inner diameter of the bed	19mm
Average diameter of glass beads	0.3mm
Average porosity	0.36 [-]
Temperature of thermostat	373K to 386K
Hydrostatic head difference	0.1mH ₂ O, 0.2mH ₂ O

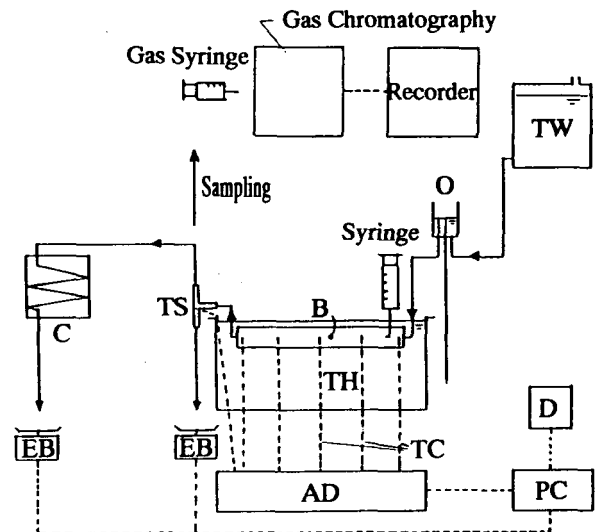


Figure 6 Schematic diagram of experimental apparatus. (C:cooler, B:packed bed, TW:water tank, TS:three-way tube, TH:thermostat, O:overflow, EB:electric balance, AD:A/D converter, D:disk unit, TC:thermocouples, PC:personal computer.)

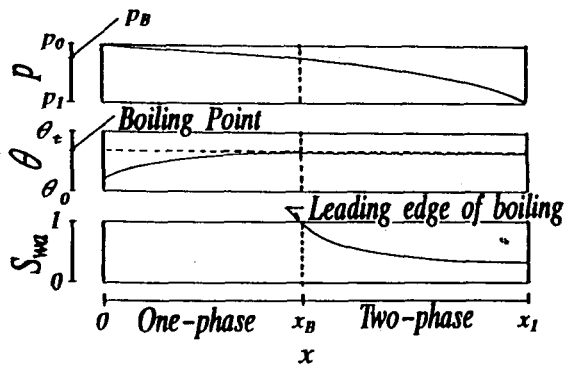


Figure 7. Illustration of numerical model.

Numerical Model

Figure 7 shows an illustration of the mathematical model. In this figure, x_B indicates the leading edge of boiling (that is, the position at which water phase starts to boil) in the water-steam flow system. Under the constant pressure gradient $(p_0 - p_B)/x_B$, water in temperature of θ_0 is injected into the bed submerged in the thermostat at a temperature θ_1 . When the water starts to boil at $x = x_B$ in the bed, the temperature of the steady state increases gradually in the region of $[0, x_B]$, and becomes the constant boiling point in $[x_B, x_1]$. Then, water saturation is equal to unity by the leading edge of boiling x_B . In the region of $[x_B, x_1]$, the saturation and the pressure are calculated by the following equations (Niibori et al., 1987, Niibori & Chida, 1991):

$$\frac{\partial}{\partial X} \{ (k_{rwa} + M k_{rga}) \frac{\partial P}{\partial X} \} = -G(\gamma - 1) \quad (16)$$

$$0 = \frac{\partial}{\partial X} (k_{rwa} \frac{\partial P}{\partial X}) \quad (17)$$

where dimensionless variables, X , G , γ , M and P are defined as follows:

$$X = x/x_1, \quad G = \{ a U (\theta_1 - \theta_f) x_1 \} / (L_v \rho_w v_w^*),$$

$$M = \mu_w / \mu_g, \quad \gamma = \rho_w / \rho_g,$$

$$P = \{ k (p - p_1) \} / (\mu_w v_w^* x_1).$$

All symbols used in this paper are listed as nomenclature at the end. This paper applies the correlation equation of the apparent permeability, Eqs.(13) and (15) to Eqs.(16) and (17).

The boundary conditions are described by

$$P = 1, \quad S_{wa} = 1, \quad \text{at } X = 0 \quad (18)$$

$$P = 0, \quad \frac{\partial S_{wa}}{\partial X} = 0, \quad \text{at } X = 1 \quad (19)$$

In regard to the mass transfer, let us assume that: (a) the tracer is injected into the water phase at the inlet; (b) the tracer vaporizes into the steam phase by boiling; (c) the mixing diffusion of the steam phase is ignored; (d) the density and the viscosity of each phase, and the mixing diffusivity and the latent heat of the water phase are constant.

These assumptions give the following equations (Niibori et al., 1992):

$$(1 - S_{wa}) \frac{\partial C_g}{\partial T} = - \frac{\partial (V_g C_g)}{\partial X} + D_a C_w \quad (20)$$

$$S_{wa} \frac{\partial C_w}{\partial T} = - \frac{\partial (V_w C_w)}{\partial X} + \frac{1}{P_e} \frac{\partial}{\partial X} S_{wa} \frac{\partial C_w}{\partial X} - D_a C_w \quad (21)$$

Dimensionless variables used above are defined as follows:

$$C_w = c_w / c_w^*, \quad C_g = y \rho / c_w^*, \quad P_e = v_w^* x_1 / E,$$

$$T = t / t^*, \quad t^* = (x_1 - x_B) \varepsilon / v_w^*, \quad V_w = v_w / v_w^*,$$

$$V_g = v_g / v_w^*, \quad D_a = K_{GT} t^* / \varepsilon,$$

$$X = (x - x_B) / (x_1 - x_B), \quad X_{IN} = -x_B / (x_1 - x_B).$$

where c_w^* is the concentration of the tracer at the inlet of the bed, y is the fraction of the tracer in the gas phase, and K_{GT} is the over-all mass transfer coefficient (Bird et al., 1960, p.654).

The boundary conditions are

$$V_w C_{w-} = V_w C_{w+} - \frac{1}{P_e} \frac{\partial C_w}{\partial X}, \quad \text{at } X = X_{IN} \quad (22)$$

$$\frac{\partial C_w}{\partial X} = 0, \quad \frac{\partial C_g}{\partial X} = 0, \quad \text{at } X = 1 \quad (23)$$

where: C_{w-} is the tracer concentration at

$$X = \lim_{\delta \rightarrow 0} (X_{IN} - \delta) = X_{IN-},$$

and C_{w+} is at

$$X = \lim_{\delta \rightarrow 0} (X_{IN} + \delta) = X_{IN+},$$

Eq.(22) is derived from the, so-called, closed vessel

assumption, which is available in a system which has larger back-mixing magnitude than that of the surrounding (Levenspiel, 1972, p.276).

The initial condition and the tracer injection are described by

$$T=0, C_w=0, C_g=0, \text{ in } X_{IN} \leq X < 1, \quad (24)$$

$$0 \leq T < T_{in}, C_w=1, \text{ at } X=X_{IN}, \quad (25)$$

$$T < 0, T_{in} < T, C_w=0, \text{ at } X=X_{IN}. \quad (26)$$

where T_{in} is the injection time of tracer.

Comparisons with the experimental data

m, x_B, G, D_a and P_e are unknown parameters in the numerical model mentioned above. Of them, m and x_B are determined from the flow rate into the bed and the temperature data in the bed, respectively. The other parameters G, D_a and P_e are estimated as follows:

(a) The value G is calculated from the steam flow rate Q_g in the steady state, because the relationship between G and Q_g is expressed by

$$G = Q_g / Q_w^*, \quad (27)$$

(Niibori & Chida, 1992), where Q_w^* is the characteristic flow rate, defined as follows:

$$Q_w^* = \pi r_{IN}^2 \rho_w v_w^*, \quad (28)$$

where r_{IN} is the inner diameter of the bed, and v_w^* is velocity of water phase, when the saturation is unity.

(b) The physical meaning of D_a is the rate constant to describe the mass transfer of tracer from the water phase to the steam phase. The transfer rate is fast enough as compared with the rate through water or steam phase. Thus, the value can be basically assumed to be infinity in this paper. However, in the numerical analysis of the mathematical model, we must set D_a large enough. Figure 8(a) shows the sensitivity of D_a on the tracer response, where W_{IN} is the dimensionless total amount of tracer, C_g is the dimensionless concentration (the gas content in the steam phase) at the outlet, and T is the dimensionless time. The sensitivity decreases, as the value of D_a larger. When the D_a is greater than 5, the response does not depend on D_a . From these calculations, the value is assumed to be 10 in the numerical analysis. For reference, Figure 8(b) shows the time-change of

C_w at the outlet in the same way as Fig.8(a). Fig.8(b) denotes that the injected tracer almost moves from the water-phase to the steam phase in the bed for case of D_a larger than 5.

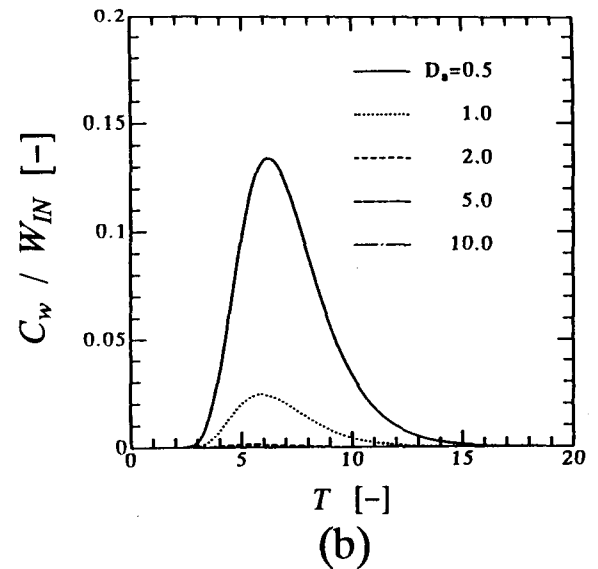
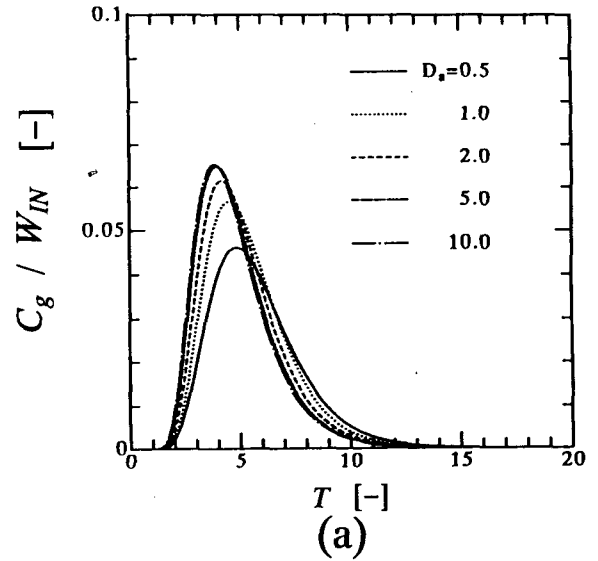


Figure 8 Sensitivity of the dimensionless, over-all mass transfer coefficient on (a) C_g and (b) C_w at the outlet. ($G = 2.5 \times 10^{-3}$, $P_e = 60$, $X_{IN} = -0.5$, $m = 4$)

(c) This paper determines the value of P_e from the tracer response in a single-phase flow system of the bed. Figure 9 denotes the tracer responses without boiling of water. The experiment (Run No.C1) is carried out in room temperature, by using the same bed. The tracer is 2cm³ of KCl solution (about 7.5mol/m³), whose concentration at the outlet is estimated by the electronic conductivity. In Fig.9, the experiment data agree quite well with the calculation of $P_e=60$.

As mentioned above, all values of the parameters are evaluated in advance. Figure 10 indicates between G and m , evaluated from the flow rate into the bed in the steady state. From this figure, we can recognize that the value of m decreases from 4 to about 3, as the value of G increases.

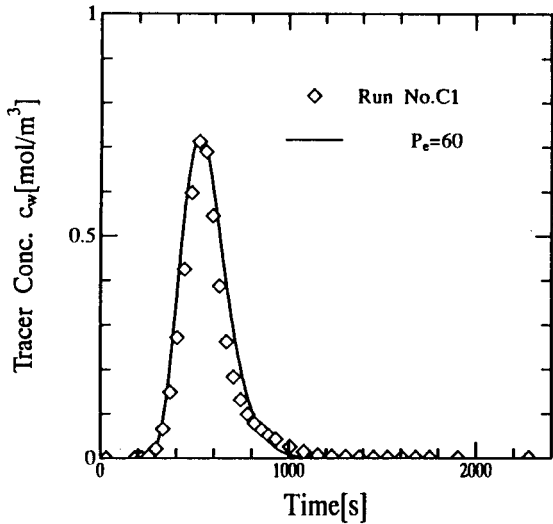


Figure 9 Evaluation of P_e .

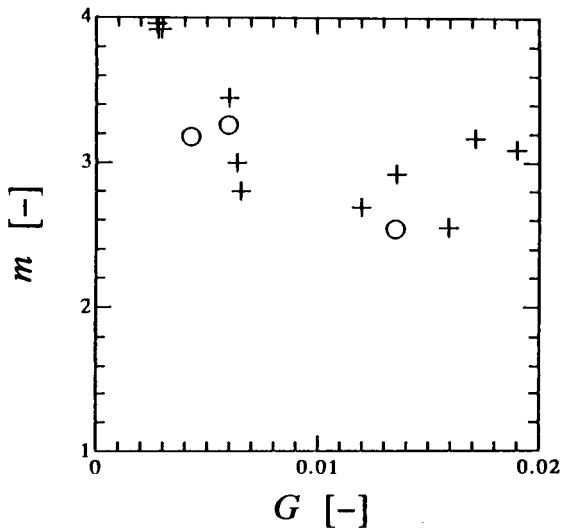


Figure 10 Relation between the dimensionless heat flow into the bed G and the value of m estimating the local distribution of saturation. (symbols o:290mm, +:145mm in length of the packed bed.)

Figure 11 shows an example of comparing the calculated results with the experiment data of tracer response. These data (Run No.31-33) are conducted at $m=3$ in Fig.10 ($G = 6 \times 10^{-3}$). The calculated value for $m=3$ agrees well with the data. The fact confirm the validity of our model. If we refer to the calculated tracer responses for $m=2$, $m=3$, and $m=4$, it is clear that the mass transfer depends

strongly on local distribution of S_w in the bed. In the same way, Figure 12 shows the data (Run No.21-24) conducted at $m=4$ in Fig.10 ($G = 3 \times 10^{-3}$). The calculated values for $m=4$ coincide with the data as well.

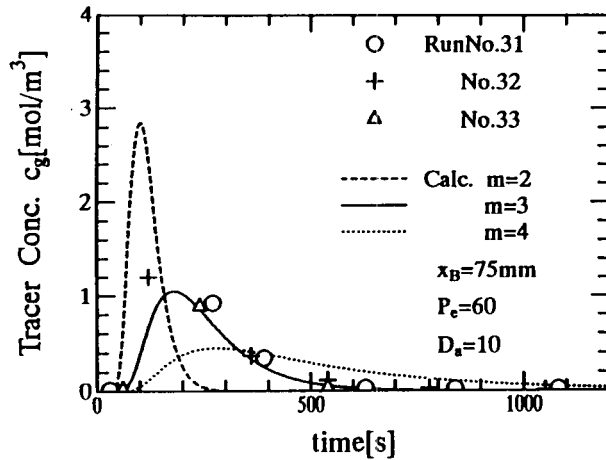


Figure 11 Comparisons of the calculated values with the experimental data conducted at $m=3$.

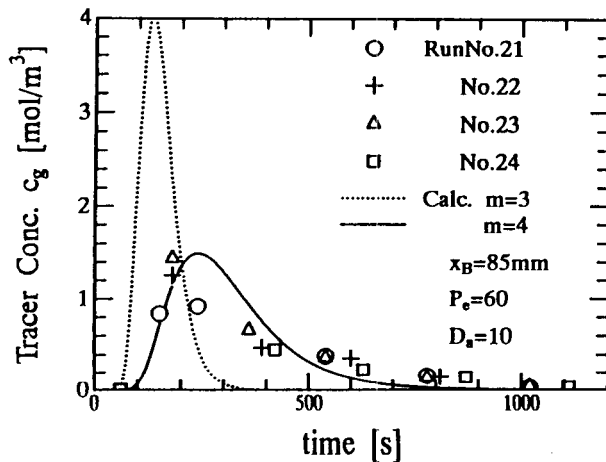


Figure 12 Comparisons of the calculated values with the experimental data conducted at $m=4$.

CONCLUSION

We discussed a model of local distribution of saturation in a fractured layer, whose detail structure is not detected. The model, based on the Bernoulli trials as a probability density function of saturation, gives correlation equations of the apparent relative permeabilities to the arithmetical mean of saturation. The equations agrees quit well with the experimental results of mass transfer in water-steam flow with boiling in a permeable medium.

NOMENCLATURE

a : specific surface area [1/m]
 c : concentration of tracer [mol/m³]
 c_w^* : concentration of tracer injected at inlet [mol/m³]
 E^w : mixing diffusivity [m²/s]
 k : permeability [m²]
 K_{TG} : over-all mass transfer coefficient [s]
 k_r : relative permeability [-]
 k_r^a : apparent relative permeability [-]
 L_v^a : latent heat [J/kg]
 p : pressure [Pa]
 Q : flow rate [kg/s]
 r_{IN} : inner diameter of the bed [m]
 S : saturation, ratio in volume [-]
 t : time [s]
 t^* : space time [s]
 U : over-all heat transfer coefficient [W/m² K]
 v : velocity [m/s]
 v_w^* : velocity of water phase, when the saturation is unity [m/s]
 W_{IN} : total amount of tracer [-]
 x : coordinate in flow direction [m]
 x_B : leading edge of boiling (position at which water phase starts to vaporize in the bed [m]
 y : fraction of tracer gas [-]
 θ : temperature [K]
 μ : viscosity [Pa s]
 ρ : density [kg/m³]
 σ : standard deviation [-]

Subscript

a : arithmetical mean
f : fluid
g : steam
t : thermostat
w : water
0 : inlet
1 : outlet

REFERENCES

- Aziz, K., and A. Settari (1979) *Petroleum Reservoir Simulation*, APPLIED SCIENCE PUBLISHERS LTD, London.
- Bird, R.B., W.E. Stewart and E.N. Lightfoot (1960) *Transport Phenomena*, JOHN WILEY & SONS, Inc., New York.
- Faust, C.R. and J.W. Mercer (1979) *Geothermal Reservoir Simulation 2: Numerical Solution Techniques for Liquid and Vapor-Dominated Hydrothermal Systems*, Water Resources Res., 15, 31-46.
- Grant, M., I.G. Donaldson, and P.F. Bixley (1982) *Geothermal Reservoir Engineering*, ACADEMIC PRESS, New York.
- Gudmundsson, J.S., A.J. Menzies and R.N. Horne (1986) Steamtube Relative Permeability Functions for Flashing Steam/Water Flow in Fractures, SPE Reservoir Eng., July, 1986, 371-377.
- Levenspiel, O. (1972) *Chemical Reaction Engineering*, Second Edition, JOHN WILEY & SONS, Inc., New York.
- Niibori, Y., Y. Ogiwara and T. Chida (1987) Effects of Phase-Change on Water-Steam Flow through a Porous Medium, J. Geothermal Res. Soc. Jpn., 9(4), 271-284.
- Niibori, Y. and T. Chida (1989) Estimations of Apparent Relative Permeabilities Considered Distribution of Saturation, J. Geothermal Res. Soc. Jpn., 11(4), 251-268.
- Niibori, Y. and T. Chida (1991) Effects of Heat Transfer on Water-Steam Flow Accompanied by Boiling in a Porous Medium, J. Geothermal Res. Soc. Jpn., 13(3), 157-166.
- Niibori, Y. and T. Chida (1992) A Consideration on the correlation equation between average saturation and relative permeabilities, J. Geothermal Res. Soc. Jpn., 14(4), 323-339 (in Japanese).
- Niibori, Y., A. Kounosu, and T. Chida (1992) Fundamental Study on Tracer Response Analysis for Water-Steam Flow Accompanied by Boiling in a Porous Medium, J. Geothermal Res., Soc., Jpn., 14(2), 129-144.
- Niibori, Y. and T. Chida (1994) Estimation Equations of Relative Permeabilities Considered Saturation Distribution, J. Geothermal Res., Soc., Jpn., to be submitted (in Japanese).
- O'Sullivan, M.J., G.S. Bodvarsson, K. Pruess and M.R. Blakeley (1985) Fluid and Heat Flow in Gas-Rich Geothermal Reservoir, Soc. Pet. Eng., J., 25, 215-226.
- Pruess, K. (1983) Heat Transfer in Fractured Geothermal Reservoirs with Boiling, Water Resources Res., 19, 201-208.
- Sorey, M.L., M.A. Grant and E. Braford (1980) Non-linear Effects in Two-Phase Flow to Well in Geothermal Reservoir, Water Resour. Res., 16, 767-777.
- Wyckoff, R.D. and H.G. Botset (1936) The Flow of Gas-Liquid Mixture through Unconsolidated Sands, Physics, 7, 325-345.
- Zyvoloski, G.A. and M.J. O'Sullivan (1980) Simulation of a Gas-Dominated, Two-Phase Geothermal Reservoir, SPEJ, 20, 52-58.